

Cognitive Internet of Vulnerable Road Users in Traffic: Predictive Neural Modulations of Road Crossing Intention

Xiaoshan Zhou,^{1*} Carol C. Menassa, F. ASCE,² and Vineet R. Kamat, F. ASCE³

¹Ph.D. Student, Dept. of Civil and Environmental Engineering, University of Michigan, Ann Arbor, MI, 48109-2125. Email: xszhou@umich.edu

²Professor, Dept. of Civil and Environmental Engineering, University of Michigan, Ann Arbor, MI, 48109-2125. Email: menassa@umich.edu

³Professor, Dept. of Civil and Environmental Engineering, University of Michigan, Ann Arbor, MI, 48109-2125. Email: vkamat@umich.edu

*Corresponding author

Abstract

Vulnerable Road Users (VRUs) such as pedestrians, bicyclists, and motorcyclists present a significant challenge for road safety due to the frequent unpredictability of their behaviors. In typical Intelligent Transportation Systems (ITS), vision-based approaches supported by networked cameras are often used to anticipate VRUs motion intentions and trajectories. However, several limitations posed by occlusions and distractions set a boundary for the efficacy of such methods. To address these challenges, this study introduces a framework that leverages data collected using wearable neurophysiological sensors on VRUs to integrate them seamlessly into the Vehicle-to-Everything (V2X) communication framework. This integration empowers VRUs to autonomously broadcast their intended movements and road usage behaviors to other road agents, especially autonomous vehicles, thereby bridging a critical gap in current vehicular communication systems. To validate this concept, we conducted an experiment involving 12 participants, from whom electroencephalogram (EEG) signals were collected as they engaged in road-crossing decisions within simulated environments. Employing Hidden Markov Models, we identified four cognitive stages intrinsic to a pedestrian's decision-making process: perception, evidence accumulation, decision resolution, and execution. Our statistical analysis further revealed significant variations in EEG activities across these stages, shedding light on the neural correlates and cognitive dynamics underpinning pedestrian road-crossing behavior. Leveraging these neurophysiological insights, we developed a predictive cognitive model using dynamic time warping and K-nearest neighbors algorithms, optimized through a data-driven sliding window approach. This model demonstrated high predictive accuracy, evidenced by an Area Under the Curve of 0.91, indicating its capability to anticipate pedestrian road-crossing actions approximately 1 second in advance of any pedestrian movement. This research not only paves the way for a novel VRU-Vehicle interaction paradigm enriched by cognitive processing for nuanced intention interpretation, but also signifies a transformative shift towards a forward-thinking and adaptive response ecosystem to mitigate road safety challenges and facilitate smoother traffic flow.

Keywords: Vulnerable road users, electroencephalogram (EEG), road-crossing intention, predictive modelling, traffic safety

1 Introduction

Autonomous driving promises to offer numerous benefits to society in terms of safety, efficiency, accessibility, and sustainability [1]. Autonomous vehicles (AVs) are equipped with advanced sensors and artificial intelligence that enable them to perceive their surroundings [2] and make safe and intelligent driving decisions [3]. Perception is the AVs' ability to interpret and understand the surrounding environment, and usually relies on computer vision techniques to complete several key subtasks, including object detection, semantic segmentation, and motion estimation [4]. In complex real-world scenarios, accurately predicting the future behavior and trajectories of moving objects poses significant challenges for ensuring the safety and reliability of autonomous driving systems [5]. This challenge is particularly pronounced when it comes to predicting pedestrians' future behaviors and trajectories [6, 7].

Pedestrians exhibit complexity of behavioral patterns in interactions with a wide range of traffic scenarios, such as jaywalking, hesitation in road-crossing, and unexpected stopping or backtracking, making them difficult to anticipate [8]. This renders them Vulnerable Road Users (VRUs) that are exposed to an increased risk of collision in traffic environments [9]. According to the Fatality Analysis Reporting System from the National Highway Traffic Safety Administration, VRUs constituted approximately 34% of individuals killed in all motor vehicle crashes [10]. The World Health Organization also reveals that half of all road traffic deaths involve VRUs [11]. This issue is even more pronounced for AVs, as VRUs can use eye contact or gestures to communicate intentions to human drivers, which are however subtle and difficult for machines to interpret [12]. Recognizing their susceptibility to severe injuries, prioritizing the safety of VRUs is crucial for enhancing overall traffic safety.

Despite research efforts to improve pedestrian detection, intent and trajectory prediction using sensor fusion and computer vision techniques [13], these algorithms face several key limitations due to environmental conditions and sensor constraints, which can lead to potential safety issues. Automated vehicles rely on sensors like cameras, LiDAR, and radar to perceive their environment, but these sensors have limitations in range, resolution, and accuracy [14]. They are susceptible to noise and errors in measuring the positions, velocities, and trajectories of pedestrians under various lighting (e.g., low light or direct sunlight) and adverse weather conditions (e.g., fog, heavy rain, or snow) [15, 16]. Advanced sensor fusion techniques partially address uncertainty in sensor measurements but require significant computational resources to process up to 5TB of data that is typically generated per hour [17] and may still fail in invisible situations, such as pedestrians occluded from view [18].

State-of-the-art research suggests using cooperative sensing in Vehicle-to-Vehicle and Vehicle-to-Infrastructure architectures [19], where cameras on other AVs or traffic signals provide a different viewpoint to detect pedestrians' location and motion, sharing this information with approaching vehicles unable to see the pedestrian due to blind spots [20]. However, this approach relies on nearby connected AVs and traffic signs

with sensing capabilities, making it ineffective in sparse vehicle areas or unsignalized crosswalks. Additionally, forecasting pedestrians' future behaviors and motion trajectories remains a complex challenge for AVs. Even detecting a pedestrian standing at the roadside does not guarantee accurate prediction of whether they intend to cross the road. The unpredictable and often abrupt nature of pedestrians' movements makes it difficult for AVs to react in time to sudden changes or unexpected crossings, raising concerns about the safety and comfort of autonomous driving systems [8].

In order to avoid collisions and ethical dilemmas for the protection of pedestrians, a crucial strategy is to focus on the upstream decision-making point to better forecast pedestrians' future behaviors and trajectories. While the development of more robust vision-based perception and pedestrian motion trajectory estimation is nearing its limits, we explore a new avenue that advances VRUs' ability to independently and directly broadcast their intended road usage behaviors to other road agents. This shift transforms the reliance on sensors—from one or multiple sources installed on vehicles for passive detection and intention prediction of VRUs—to a proactive and more direct approach. Enabled by wearable neurophysiological sensing, the proposed method captures nuanced cognitive activities in real-time and interprets future movements from predictive neural modulations. By allowing VRUs to actively participate in the Vehicle-to-Everything (V2X) architecture, intentions regarding future interactions between VRUs and AVs can be communicated [21]. AVs can then optimize their route and velocity based on more precise and real-time VRUs' road usage demand while ensuring the safety of all road agents. We refer to this concept as the "Beacon Network of VRUs."

This work aims to establish a proof-of-concept for this neuro-biosensor-enabled intended road usage behavior interpretation. Preliminary results derived from the designed experiment offer insights that will serve as key references for feature and channel selection to convert this concept into an affordable real-world neurosensing application. The remainder of this paper is structured as follows: Section 2 provides a review of related literature. Section 3 introduces the experimental design, data collection, and analysis pipeline. Section 4 reports the results. Associated discussions and practical implications are presented in Section 5. Finally, Section 6 concludes the paper and highlights future research directions.

2 Literature Review

This section first reviews vision-based modalities and associated methods for detecting, tracking, and predicting pedestrian trajectories. It then presents the limitations of these methods in terms of degradation in adverse weather conditions, significant computational resource demands, and visibility and uncertainty issues. Next, it considers the potential of VRUs as active data sources within V2X frameworks, leveraging sensors embedded in smartphones to detect exact positions and motion changes. However, these methods often provide post hoc data that fail to predictively capture the dynamic and unpredictable behavioral patterns of pedestrians. Finally, we provide the rationale for using neuro-sensors and developing a brainwave-driven

computational intelligence approach to predict individuals' road-crossing intentions and discuss the technical and methodological challenges in developing such a wearable device.

2.1 Pedestrian Trajectory Forecasting

2.1.1 Vision-Based Approaches

Predicting pedestrians' future motions is essential for services like pedestrian-vehicle collision warnings, which alert drivers approaching intersections or unsignalized crosswalks by anticipating pedestrians' crossing intentions [22]. Previous research has predominantly relied on vision-based methods, utilizing road security cameras [23] or stereo-based cameras installed in passenger vehicles [13] to detect pedestrians [24], extract their behavioral features from video footage [25], and analyze collision risks between pedestrians and vehicles [26]. However, the existing vision-based methods have limitations, particularly in their ability to generalize to all crowd behaviors and traffic scenarios. These methods typically treat the intention prediction for VRUs as a dynamical motion modeling problem, often addressed using Bayesian filters [27, 28]. While effective in certain contexts, these approaches require explicit modeling of agents under specific traffic scenarios [29], which can be challenging due to the non-linearity or uncertain dynamics of VRUs over longer time periods, particularly in scenarios involving sudden path changes due to intentions to cross the road or change lanes, or interactions with other pedestrians and vehicles trajectories.

Moving forward, researchers are exploring planning-based models for forecasting pedestrians' trajectories. These models utilize inferred end goals and occupancy grid maps of the environment to generate a probability distribution over possible trajectories [30, 31]. Planning-based models do not require explicit modeling of motion dynamics, but they are limited by their reliance on a prior known end goal. Some other researchers are incorporating deep learning methods, such as three-dimensional pose estimation of pedestrians [22] or recurrent neural network-based methods that use past positions to predict future motion trajectories [32-34]. Additionally, some models incorporate contextual environment information, such as pedestrians' distance to the curb of a road and the relative locations of nearby approaching vehicles, to predict their road-crossing intentions [35, 36].

Although these data-driven methods have shown improved applicability in intention prediction, they still struggle to account for the inherent uncertainty of VRUs' planned actions. For example, a pedestrian may suddenly change direction, stop unexpectedly, or exhibit hesitation before crossing a road [8]. These actions are challenging to predict solely based on historical data or environmental cues. Additionally, interactions between multiple VRUs and vehicles further increase the complexity and uncertainty of their actions. Closing these gaps in intention prediction accuracy and robustness remains a critical challenge in pedestrian trajectory forecasting for intelligent transportation systems and autonomous driving.

2.1.2 Limitations of Vision-Based Methods

The limitations of the vision-based methods for predicting VRU intentions are summarized in the paragraphs below:

1. Adverse weather: Vision-based methods rely on sensors to detect pedestrians and accurately localize their positions. However, environmental factors such as weather and lighting conditions can significantly degrade the perceiving performance of these sensors. While sensor fusion techniques with Lidar data streams can improve accuracy [37], they are often cost-prohibitive and computationally intensive.

2. Visibility: A critical issue leading to VRUs' collisions is their invisibility when obscured by obstacles such as parked vehicles. To mitigate this, the concept of cooperative sensing has been proposed [19]. In this approach, a connected AV on the opposite side of an intersection, capable of detecting the VRU, shares information about the VRU's location and motion with the approaching vehicle. However, this cooperative Vehicle-to-Vehicle (V2V) framework has limitations. It depends on the presence of nearby connected vehicles with sensing capabilities, which may be ineffective in sparse traffic or when there are no oncoming vehicles to provide different viewpoints.

3. Uncertainty in Intention Prediction: Predicting VRUs' future motion intentions remains challenging for AVs. Even when detecting a pedestrian standing at the roadside, it is hard to estimate whether and when the pedestrian intends to cross the road. Environmental factors and the explicit representation of pedestrian behaviors (e.g., past positions, skeletal poses) are limited in predicting behavioral dynamics due to pedestrians' unpredictable nature. Researchers are exploring multimodality analysis [38] and vision-enabled body skeleton [39] or gait analysis [40] to reduce uncertainty. However, these methods may still struggle to capture hesitation and sudden changes in VRUs' future road usage behaviors.

2.2 Incorporation of VRUs in V2X

2.2.1 VRUs as Data Sources

Current collision prevention methods between vehicles and pedestrians are predominantly car-centric, relying on various sensors within the vehicle to detect and track pedestrians. However, a major limitation of these approaches is their inability to detect pedestrians in blind-spot scenarios. To address this limitation, a cooperative approach has been proposed, where pedestrians themselves can exchange information with vehicles, augmenting the car's sensor capabilities.

Cooperative approaches typically utilize smartphones as a platform for pedestrian interaction. For instance, one study used GPS in smartphones to provide exact location information, improving system accuracy and reducing reliance on external cameras for

position estimation [41]. Another study incorporated an acceleration sensor in mobile phones to detect changes in pedestrian movements, enhancing tracking accuracy [42]. In a related study, inertial smartphone sensors were used to detect changes in pedestrian movements, such as turning or crossing an intersection [43]. Researchers have also developed algorithms using wearable inertial measurement units mounted on the human body for pedestrian localization [44]. Additionally, radio signal propagation methods have been used to calculate the exact distance between vehicles and pedestrians [45]. One particular study explored using smartphones to notify nearby AVs about pedestrian positions, proposing a system architecture for pedestrian-to-vehicle communication [46]. This system further calculates collision risk and triggers alarms if necessary [47].

Although these approaches provide more accurate positional information of pedestrians and overcome measurement errors from external sensors, they are limited in their ability to capture intentions. VRUs are dynamic and exhibit unpredictable behaviors, making direct incorporation of their handheld devices as data sources beneficial. However, current research in this area predominantly relies on post-hoc analysis, capturing data only after events have occurred, which does not provide AVs with sufficient advance notice to respond effectively. Therefore, there is a gap in the research regarding methods that can capture and interpret VRUs' intentions for future motion forecasting to give AVs more time to react, thus potentially enhancing the safety and efficiency of road systems.

2.2.2 Rationale for Using Neuro-Sensors for Pedestrian Intention Forecasting

Predicting pedestrian intentions is crucial for enhancing road safety, and neuro-biosensors offer a unique approach in this regard. Recent advances in neuro-sensors have been shown to be capable of capturing instant cognitive fluctuations [48] going beyond mere psychological or emotional arousal monitoring to the interpretation of more nuanced cognitive activities, thus offering significant promise for the motivated application of predicting VRUs' future road usage behaviors. Furthermore, compared to other biosensors that generally capture physiological responses only after events occur (post-hoc), neural sensing uniquely allows for the capture of predictive neural modulations that can forecast future movements. For instance, prior studies, as referenced in [49-51], have observed and characterized brain activities that mediate between perception and action during decision-making. More specifically, empirical findings from [52, 53] reveal that during the formation of decisions, the contralateral premotor cortex accumulates evidence and exhibits dynamic activity patterns that precede the initiation of a response. Given the abundant evidence on modulatory cortical activities during perception and decision-making, there is thus a compelling rationale to develop a brainwave-driven computational intelligence approach for predicting individuals' road-crossing intentions.

Various noninvasive neuro sensing methods, such as functional magnetic resonance

imaging (fMRI), near-infrared spectroscopy (NIRS), electroencephalography (EEG), and magnetoencephalography (MEG), provide opportunities to record brain signals from the scalp. These methods can collect data seamlessly making them ideal for daily usage, removing the high surgical risk to implant invasive microelectrodes. Choosing the optimal modality to capture brain signals involves considering factors such as temporal and spatial resolution, commercial availability, and portability. Among these modalities, EEG has emerged as the most prevalent noninvasive modality in Brain-Computer Interface (BCI) experiments. In contrast, both MEG and fMRI have high costs and lack portability, limiting them to clinical settings; NIRS, while noninvasive, has critical limitations in temporal resolution, with hemodynamic responses having a 4-5 second delay [54]. EEG, on the other hand, offers outstanding temporal resolution, capable of capturing amplified electrical charges produced by brain cells in milliseconds [55]. This study leverages these features and further develops methods and establishes a proof-of-concept for analyzing the variations in neural activity to infer underlying cognitive processes and predict future motions.

2.3 Gaps in Using Neuro-Sensors to Predict VRUs' Road Crossing Intentions

2.3.1 Feature Selection for Reliable Brain Signal Classification

Developing a brainwave-driven computational intelligence approach for predicting individuals' road-cross intentions faces the initial challenge of distinguishing brain signals associated with road-cross intentions. Previous BCI experiments have revealed that around 15%–30% of participants demonstrate limited capability in generating distinct and consistent brain activities during task completion [56]. One effective strategy for addressing this challenge of “BCI illiteracy” and improving the reliability of brain signal classification is through feature selection and recording site optimization [57].

Brain signal features exhibit complex spectral-spatial patterns. Spectral patterns, especially after transformation to power, convey different information in each frequency band [58]. Spatially, EEG modalities can monitor cortex activity in the contralateral hemisphere, but precise localization for optimal site selection for the studied task can be highly beneficial. Analyzing signals from a single channel is much simpler and reduces the development cost for a real-world EEG headset product. On the contrary, multi-channel analysis requires sophisticated algorithms to process such a high-dimensional EEG feature set [59], which can lead to overfitting and excessive learning times. Therefore, this study aims to identify optimal channel and spectral characteristics to serve as key references for feature selection in future implementations of a brainwave-driven prediction system in VRUs.

2.3.2 Complexity of Cognitive Processes for Road Crossing and Underlying Brain Activities

Road crossing decisions involve a multifaceted cognitive process. Drawing upon the psychological Perception-Action model [60, 61], the cognitive states underlying the

road crossing activity include perceiving the environment (especially selectively attending to key information, such as oncoming traffic), assessing the risk based on the speed and distance of vehicles, determining the available time to cross, making the decision to cross or not, and finally, initiating the crossing by stepping onto the road and walking to the other side. These processes are complex and involve multiple high-level cognitive functions, particularly selective attention and working memory.

Selective attention is responsible for orienting attention to relevant environmental information, especially threatening cues, while ignoring irrelevant stimuli [62]. This process is controlled top-down, with attention reorientation to appropriate stimulus features initiated from dorsal frontoparietal regions [63]. This cognitive control heavily relies on the prefrontal cortex; meanwhile, some neuroimaging literature also emphasizes the interplay between the prefrontal and parietal cortices to exchange the sensory information and code the attributes of the expected stimulus with anticipatory perception [64, 65].

Working memory is responsible for temporarily holding and manipulating information essential for decision-making, planning, and memory retrieval. Multiple cortical regions are implicated in working memory tasks. The prefrontal cortex plays a crucial role in rule-based response selection. In contrast, the ventrolateral cortex is responsible for the active maintenance of information in rule-based learning and long-term memory retrieval [66]. Additionally, previous studies have identified that the connectivity patterns in right parietal-occipital regions are closely related to the quality of visual working memory [67].

However, these pieces of evidence from neurophysiological studies are often based on using simple icons as experimental stimuli. The cognitive processes involved in real-life scenarios, such as road-crossing behaviors, and the modulated preparatory neural activities preceding such road-crossing decisions, remain unclear. This study aims to provide empirical evidence to shed light on how key cognitive functions, such as working memory and selective attention, are combined to contribute to the decision of whether to cross the road or not. A comprehensive investigation of brain activation patterns is conducted to uncover the neurophysiological signatures underlying road-crossing intentions. This research also provides valuable references for feature selection in the brainwave-driven computational model for predicting pedestrians' road-crossing intentions.

3 Research Methodology

3.1 Participants

Twelve individuals participated in the designed experiment (six males and six females; mean age of 24.92 years). Any interested individuals aged between 18 and 45 years old and having a normal or corrected-to-normal vision were eligible to participate and indicate their willingness to the research group. The selected individuals then received

an electronic version of informed consent that notified them about the experimental protocol and any preparatory requirements. The research team addressed any questions brought up by the participants. If they provided their informed consent before the experiment, the participants were assigned a random number and their personal contact information (including name, email address) was deleted. All participants reported not having a history of neurological health issues, such as epilepsy or brain cancer. They received 25 dollars per hour as compensation for their participation in this experiment. This study was approved by the Institutional Review Board from the University of Michigan (Reference ID HUM00249262).

3.2 Stimuli

The stimuli for this study were carefully designed to simulate a variety of traffic conditions and scenarios, reflecting real-world complexities. Drawing on prior research highlighting that 30% of pedestrian accidents occur at non-signalized crosswalks [68-71], and building upon studies that examine pedestrian intentions at intersections [22, 37, 72], we developed five scenarios. These scenarios are designed to represent hazardous situations commonly encountered at different traffic volumes and environmental settings, as described in Table 1. The stimuli, which were crafted using Adobe Animate and are illustrated in Figures 1-4, range from low to high traffic conditions at non-signalized crosswalk areas and include intersections within residential zones, each presenting unique characteristics and challenges for the pedestrian. This careful selection and design of stimuli aim to ensure the scenarios are as lifelike and relevant as possible, facilitating an accurate study of pedestrian behavior under varied traffic conditions.

Table 1 Descriptions of the simulated experimental scenarios

Traffic volumes	Description
None	A two-lane road without signalized crosswalks, with no cars approaching within sight.
Sparse	A two-lane road without signalized crosswalks, with two cars approaching at a slow speed within sight.
Busy	A two-lane road without signalized crosswalks, with two cars approaching in the adjacent lane and three vehicles approaching in the opposite lane at a moderate speed within sight.
Surface-marked	A four-way intersection with surface-marked crosswalks but without traffic lights. One car is waiting behind the sidewalk on the side opposite to the pedestrian's intended movement, with its left-turn signal flashing and visible within sight.
Signalized	A four-way intersection with surface-marked crosswalks and a traffic light (green/red). One car is waiting behind the sidewalk in the vertical orthogonal direction relative to the pedestrian's intended movement with its left-turn signal flashing. A red traffic light, perpendicular to the pedestrian's movement, is visible at the intersection.

The animations were presented to the participants through PsychoPy (version 2022.2.5). PsychoPy [73] is an open-source software package for use in neuroscience and experimental psychology research and was chosen for its robustness in presenting visual stimuli and capturing real-time behavioral responses, ensuring high fidelity in the representation of each animated scenario and consistency in participants' experiences across the study.



Figure 1. The “None” scenario to simulate road-crossing intention.



Figure 2. The “Busy” scenario to simulate road-crossing intention.



Figure 3. The “Surface-marked” scenario to simulate road-crossing intention.



Figure 4. The “Signalized” scenario to simulate road-crossing intention.

3.3 Experimental Procedure

One day before the experiment, the participants received a reminder email about the experimental appointment and preparatory requirements, including ensuring a good night's sleep, abstaining from caffeinated beverages, and showering with a mild shampoo before the experiment. On the day of the experiment, the participants were invited to enter the laboratory, which was a dimly lit and sound-attenuated room to begin the experiment. First, the participants were asked to fill out a self-report questionnaire to collect basic demographic information (such as age, gender, race, education level). Then the experimenter assisted the participants in wearing the EEG headset (details about the headset are covered in section 3.4). Saline-soaked felt pads were used for electrode contact. After fitting the headset, careful adjustments were made to each channel to optimize electrode-skin contact. This involved separating hair to ensure adequate contact with the scalp and rehydrating the sensor felts as necessary. The quality of contact for each electrode was monitored through a software interface, which displayed real-time feedback on the connection quality. Recording of EEG signals started only after ensuring that all electrodes maintained optimal contact quality, thereby guaranteeing the integrity and reliability of the captured data.

The formal experiment consisted of five trials as described in Section 3.2. Each trial began with a cross (+) showing at the center of the monitor screen and lasting for 500ms. This setting has been commonly used in visual stimuli based psychological experiments to calibrate the participants' attention to the center of the screen. 500-800 ms was usually adopted as a reasonable time period as a too short duration may not be visible but a too long one might distract from further official stimuli. Then a video clip depicting a simulated road-crossing scenario (as shown in Figure 5) was played. Participants were instructed to envision themselves as the pedestrian standing beside the road. Their task was to perceive the traffic flow and determine the safest moment to cross the road. When they decided it was the right moment to cross, they pressed the "up" key on the keyboard. To ensure that each trial was completed, every animation continued in a loop until the participant responded, guaranteeing a cross decision for each scenario. Following this, participants provided a retrospective thinking aloud, reflecting on how they perceived and made decisions in each of the five scenarios.

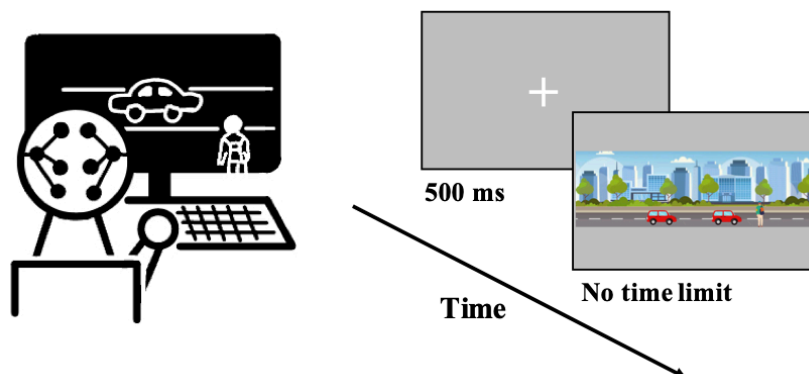


Figure 5. Illustration of the experimental procedure.

3.4 EEG Recording

EEG signals were collected with a 14-channel electrode cap according to the international 10-20 system (EPOC X, Emotiv). The sampling rate was 128Hz. The bandwidth of the recorded signals ranged from 0.16Hz to 43Hz. The configurations of the 14-channel electrodes (as shown in Figure 6) and their corresponding cortical regions are: the frontal region (AF3, F7, F3, F4, F8, AF4), responsible for executive functions including decision-making, problem-solving, and planning; the central region (FC5, FC6), implicated in integrating sensory and motor information; the parietal region (P7, P8), key to spatial awareness and processing of visual and somatosensory data; the temporal region (T7, T8), essential for semantic processing and memory functions; and the occipital region (O1, O2), dedicated to visual processing.

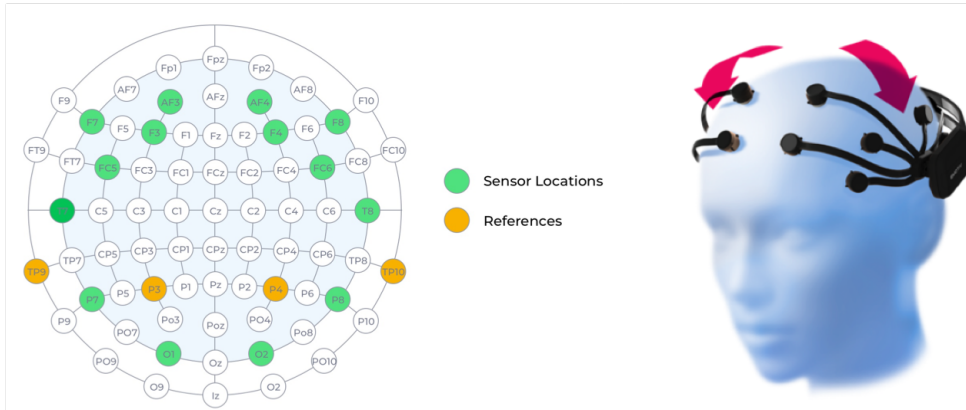


Figure 6. The configurations of the 14 channels in the EPOC X used in our study [74].

3.5 Data Analysis

Given the complexities of perceptual decision-making involved in road crossing, we adopted a data-driven approach to identify the underlying neurophysiological signatures associated with these subtle mental processes. This approach utilized statistical inference methods to analyze variations in EEG power across various features (70 channel and frequency band combinations), identifying the cognitive processes predominant at different stages of decision-making. To construct the training dataset, we implemented a sliding window technique. Subsequently, we developed a novel machine learning method (see section 3.5.5) designed to precisely predict the moment when individuals decide to initiate road crossing.

3.5.1 Time-frequency Analysis and Segmentation

The time-frequency analyses of the EEG signals were conducted using the EmotivPRO v3.0 software [75]. Each trial was transformed in the frequency domain using a Fast Fourier Transform analysis [76]. Subsequently, EEG power spectra were extracted for five key frequency bands: theta (4–8 Hz), alpha (8–12 Hz), low beta (12–16 Hz), high beta (16–25Hz) and gamma (25–45 Hz) at a sampling rate of 8Hz, aligning with the temporal resolution necessary for capturing the cognitive dynamics underlying our studied task. Then, the segmentation of EEG data was performed from the onset of each stimulus presentation to the moment a participant responded by pressing a key on a trial

basis.

3.5.2 Latent Cognitive Stages Identification with Hidden Markov Model

The primary objective of this analysis was to uncover latent stages in the cognitive processes involved in making road-crossing decisions, using EEG data recorded from 14 channels and spanning five distinct frequency bands. This resulted in a dataset comprising seventy features for each timestamp. Given the high dimensionality of the data, our initial step was dimensionality reduction to distill the essential features while preserving the variance inherent in the dataset. To achieve this, we employed Principal Component Analysis (PCA) [77], a statistical procedure that utilizes orthogonal transformation to convert possibly correlated variables into a set of linearly uncorrelated variables known as principal components. This technique was applied to the dataset to extract the top five principal components, expected to capture the majority of the variance within the data while significantly reducing its dimensionality of the feature spaces. This reduction facilitates more efficient processing in subsequent analyses.

Subsequently, to explore the temporal dynamics and identify the underlying latent stages during the road crossing decision-making from the EEG data, we utilized a Hidden Markov Model (HMM). The HMM is a statistical model that assumes the system being modeled is a Markov process with unobserved (hidden) states [78]. HMMs are particularly well-suited for time series data where the goal is to infer the hidden state sequence from the observable data. In our context, the observable data are the principal components derived from the EEG recordings, and the hidden states are the latent cognitive stages we aim to uncover.

To parameterize the HMM, we specified the number of latent states in the model to be four, reflecting the hypothesized stages participants may transition through during the decision-making: selective attention to perceptual cues, evidence accumulation, reaching decision resolution, and executing the action. The model then estimated several key parameters: the distribution of initial states across the dataset, the probabilities of transitioning from one state to another (state transition matrix), and the parameters of the Gaussian distributions associated with each latent state. These Gaussian distributions model the expected distribution of the data when the system is in each of the respective hidden states.

The process of estimating these model parameters was performed through a fitting procedure, wherein the model iteratively adjusted the parameters to maximize the likelihood of the observed data given the model structure. This iterative process continued until convergence, ensuring that the model parameters were optimized to best represent the underlying structure of the EEG data.

Following the optimization of the model parameters, we applied a state prediction procedure on the dataset. This step involved using the optimized model to infer the most

likely sequence of hidden states throughout the time series, based on the observed data. The inferred sequence of states provided us with a temporal map of the latent cognitive stages experienced by participants, as reflected by the EEG recordings. The analysis of these latent stages and their transitions offered novel insights into the cognitive processes underlying the road-crossing decision-making.

3.5.3 Statistical Analysis of EEG Power Across Different Latent Cognitive Stages

Following the identification of latent stages via HMM, we segmented the EEG data sequences accordingly, assigning labels to each segment reflecting its corresponding latent stage. We then extracted these segments, detected and removed outliers based on the Interquartile Range (IQR) method, and computed the mean EEG data under each identified latent stage. This process allowed us to quantitatively characterize the EEG activity associated with different cognitive states elicited across subjects.

Before conducting inferential statistics, we assessed the normality of the data distributions for each latent stage across scenarios. This normality check was performed using the Shapiro-Wilk test. Our analysis indicated that the normality assumption was not met (p value > 0.05). Thus, we opted for Friedman's Analysis of variance (ANOVA)—a non-parametric alternative to repeated measures ANOVA—to identify statistically significant differences in EEG data elicited under each latent stage across subjects. Following a significant result (p value < 0.05) in Friedman's ANOVA, we conducted post-hoc tests to pinpoint specific pairwise comparisons that contributed to the overall significant differences detected by the Friedman test.

3.5.4 Sequence Segmentation with A Sliding Window and Oversampling

To capture the temporal dynamics of cognitive processes, a sliding window approach was adopted to extract sequential data points. Each window, with a predetermined length and stride, incrementally increases by 0.125s from 0.25s to 2s, traverses the EEG sequence to carve out segments for further analysis (as illustrated in Figure 7). The length of the window determines the size of each segment, capturing a fixed duration of EEG activity, while the stride—the step size with which the window is moved—controls the overlap between consecutive segments. The label assignment strategy is designed to distinguish the segments that reach the end of a sequence instance, signifying the final intention resolution and execution of crossing the road, by assigning them a label of '1'. This method ensures that each segment is contextually anchored, thereby facilitating an understanding of the sequential patterns inherent in the EEG data.

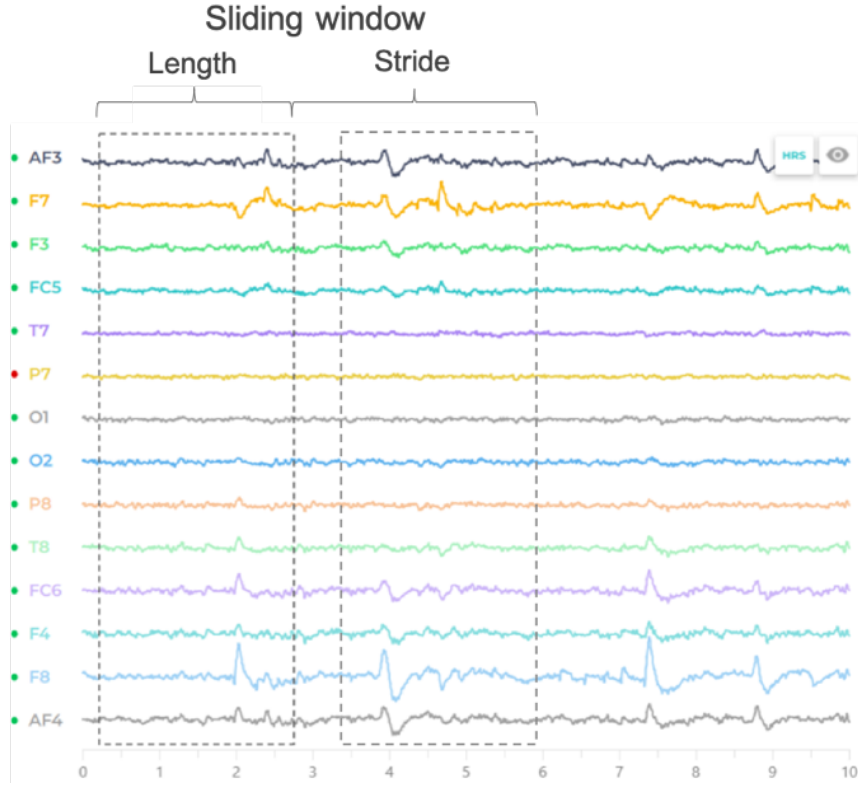


Figure 7. Illustration of the sliding window traversing EEG signals with a predetermined length and stride.

Given the pronounced class imbalance within our dataset, with a scarcity of instances belonging to the minority class “1”, we employed the Adaptive Synthetic Sampling Approach (ADASYN) for oversampling. ADASYN is distinguished by its ability to adaptively generate synthetic samples near the borderline than the interior of the minority class [79]. This strategy is particularly advantageous for our study as it enriches the minority class with examples that are likely to be more challenging for classifiers to learn, thus potentially enhancing the model's ability to generalize from underrepresented patterns in the data.

3.5.5 Classification

We developed machine learning models to predict the precise moments when participants decide to initiate road crossing. This was achieved by classifying sequences that were crafted and labeled in the previous step. For this classification, we utilized a K-Nearest Neighbors (KNN) classifier augmented with Dynamic Time Warping (DTW) [80]. DTW is a robust algorithm designed to measure similarity between two temporal sequences. It allows for elastic transformations of the time axis, accommodating varying speeds in the data patterns which is particularly advantageous for EEG data, where similar cognitive processes may unfold at different rates across instances. The following principals explain how DTW can compare two time series by optimally aligning their points to minimize the distance between them, thus taking into account the temporal differences in speed or duration between the series.

Two sequences that we want to compare are defined below:

- $X = [x_1, x_2, \dots, x_n]$ with length n
- $Y = [y_1, y_2, \dots, y_m]$ with length m

The goal of DTW is to find a path through the grid that defines the mapping between X and Y that minimizes the total distance between the aligned elements of the sequences. This path is known as the "warping path."

Step 1: Constructing the Distance Matrix

First, we compute the distance matrix D , where each element $D(i, j)$ represents the distance between x_i and y_j . The choice of distance metric can vary, but a common choice is the Euclidean distance:

$$D(i, j) = (x_i - y_j)^2$$

Step 2: Accumulated Cost Matrix

Next, we calculate the accumulated cost matrix C using dynamic programming. Each element $C(i, j)$ represents the minimum cumulative distance to align the first i elements of X and the first j elements of Y . The accumulated cost matrix is defined as:

$$C(i, j) = D(i, j) + \min \{C(i-1, j-1), C(i-1, j), C(i, j-1)\}$$

The boundary conditions are:

$$C(0, 0) = D(0, 0)$$

$$C(i, 0) = D(i, 0) + C(i-1, 0) \text{ for } i = 1, 2, \dots, n$$

$$C(0, j) = D(0, j) + C(0, j-1) \text{ for } j = 1, 2, \dots, m$$

Step 3: Finding the Optimal Warping Path

The optimal warping path P is the path from $C(n, m)$ to $C(0, 0)$ that minimizes the total cumulative distance. This path can be found by starting at $C(n, m)$ and tracing back to $C(0, 0)$ by moving through the indices that provide the minimum accumulated cost as defined above.

Step 4: Calculating the Total Cost

The total cost of the optimal warping path, which is the measure of similarity between X and Y , is given by the value of $C(n, m)$.

By integrating DTW as the distance metric, our KNN classifier gains the flexibility to accurately measure the similarity between EEG sequences, making it well-suited for recognizing complex, temporally varying patterns associated with different cognitive states within time series data. The KNN algorithm determines the classification of a sample by identifying the majority class among its k closest neighbors. Through tuning, we have chosen $k = 5$ to strike a balance that enables pattern recognition while maintaining its generalizability.

To assess the performance of our classifier, we implemented a five-fold cross validation approach. This technique divides the dataset into five subsets. In each validation cycle, four subsets underwent ADASYN oversampling to address class

imbalance before being used for training, while the fifth subset is reserved for testing. Each subset of data is used for testing exactly once, and we calculated and reported the average of the evaluation metrics across all subsets. Given the challenges posed by class imbalances and the inherent temporal complexity of EEG data, we selected accuracy, precision, recall, and the F1 score as metrics to measure the model's predictive performance comprehensively.

4 Experimental Results and Analyses

4.1 Behavioral Response Time

The violin plots (Figure 8) show the distribution and probability density of the subjects' response times across the five traffic scenarios. In the "None" scenario, where no traffic was present, the mean response time was 4.02 seconds, with a 95% Highest Density Interval (HDI) ranging from approximately 1.91 to 7.04 seconds.

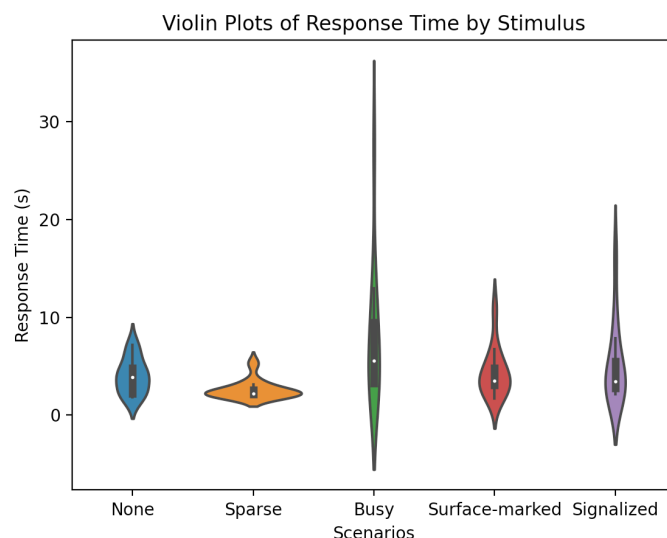


Figure 8. Violin plots of response time by stimulus

This variability suggests a diverse approach to the timing of crossing an empty road, which potentially presented an unexpectedly complex decision-making environment due to the lack of traffic cues. The "Sparse" traffic scenario yielded a shorter mean response time of 2.62 seconds and a narrower 95% HDI from about 2.07 to 4.76 seconds, suggesting that subjects could make more decisive actions with less hesitation. The "Busy" scenario elicited a prolonged mean response time of 8.08 seconds, with a considerably wider 95% HDI of 3.17 to 23.53 seconds. This indicates a more cautious approach by subjects, reflecting the increased difficulty and hesitation subjects faced when navigating dense traffic.

The 'Surface-marked' scenario recorded a mean response time of 4.36 seconds, with a 95% HDI ranging from 1.79 to 9.73 seconds. Insights obtained from subjects during retrospective think-aloud sessions revealed that additional time was allocated to ensure

that the signalized turning vehicle would wait behind the stop line, allowing pedestrians to cross first. This added level of precaution reflects the uncertainty pedestrians feel, in contrast to the 'Sparse' scenario, where the oncoming car's motion provides clearer indications of driver behavior, reducing ambiguity regarding the moment the vehicle will pass by.

In the 'Signalized' scenario, subjects took an average of 5.27 seconds to decide to cross, with a 95% HDI between 2.23 and 14.59 seconds. Traffic signals are expected to alleviate some of the cognitive burden on pedestrians. However, as reflected in the response times, subjects took additional time to interpret the traffic lights. Moreover, subjects may also perceive an increased risk due to the possibility of signal changes and the potential for drivers to disobey the signals, leading to greater caution and a reliance on their own judgment despite explicit traffic cues. This suggests that in environments where control mechanisms (like traffic signals) are absent, pedestrians may switch to a simpler heuristic strategy, which can sometimes result in faster decision-making processes.

4.2 Latent Stages Underlying Road-Crossing Decision-Making

In exploring the cognitive processes associated with road-crossing decisions, PCA and HMMs were applied to the EEG data. Figure 9 shows the feature reduction and explained variance from the dataset from a subject in making road-crossing decision under the 'Sparse' traffic scenario. The components are ordered by their ability to capture the variability within the data, with the first component accounting for the highest variance.

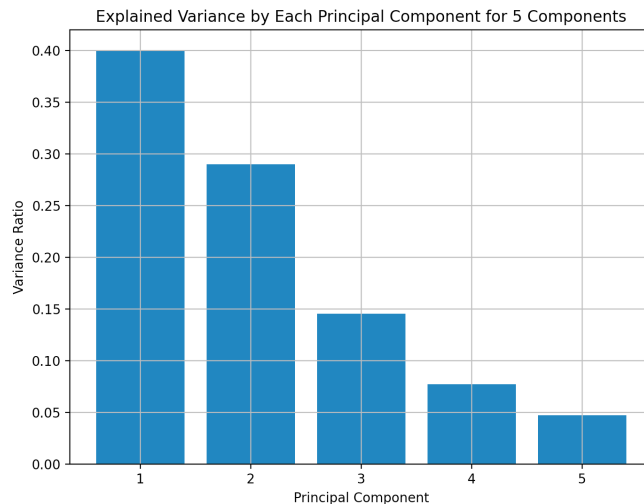


Figure 9. Bar chart illustrating the proportion of variance explained by each of the first five principal components obtained from PCA of EEG data.

According to Figure 9, the first five components cumulatively capture the majority of the variance, approximately 94%. The first two principal components accounted for nearly 70% of the variance within the data. This substantial coverage of variance

validates our choice to retain these components for further analysis, ensuring a comprehensive representation of the data in our study.

Upon reducing the dimensionality, an HMM was applied to the five retained principal components to model the temporal structure of the EEG data and to discover latent stages. The HMM visualization (Figure 10) presents the state transitions over time across the five dimensions. Four distinct states were inferred, each potentially corresponding to a unique cognitive phase in the decision-making process. The shaded areas in the time-series plots indicate the duration of each state, illustrating the dynamic switching behavior of the subject's cognitive states throughout the decision-making process.

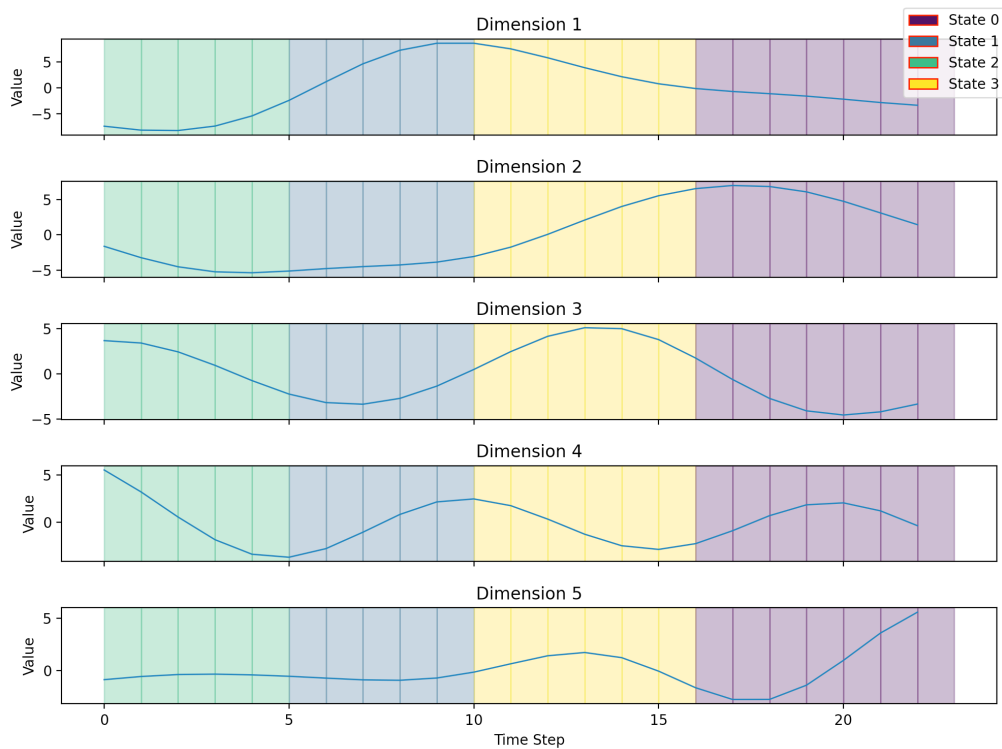


Figure 10. State transitions identified by HMM. Note: the hypothesized four stages underlying the perceptual-decision making for road crossing are: selective attention to perceptual cues, evidence accumulation, reaching decision resolution, and executing the action.

4.3 EEG Power Variations Across Latent Stages

In the last subsection, HMMs provided a detailed quantitative analysis of the temporal progression in cognitive states as subjects approached the decision-making process of crossing a road. This analysis revealed intricate patterns that reflect the mental processes involved in decision-making, suggesting distinct phases of sensory processing, attention allocation, and planning. To further understand the neurophysiological underpinnings and the cognitive dynamics associated with these discerned stages, we applied HMMs across different scenarios for all subjects to

identify and label latent stages. Subsequently, outliers were identified in each EEG data sequence using the IQR, calculated as the difference between the 25th (Q1) and 75th (Q3) percentiles. Data points outside the range of $Q1 - 1.5 \times IQR$ and $Q3 + 1.5 \times IQR$ were classified as outliers and excluded to improve the reliability of our subsequent data analyses. Aggregated EEG power data, cleared of outliers, from the four latent stages, is depicted in Figure 11. Using these structured data, we performed Friedman's ANOVA to evaluate potential differences in EEG power across the various cognitive stages identified.

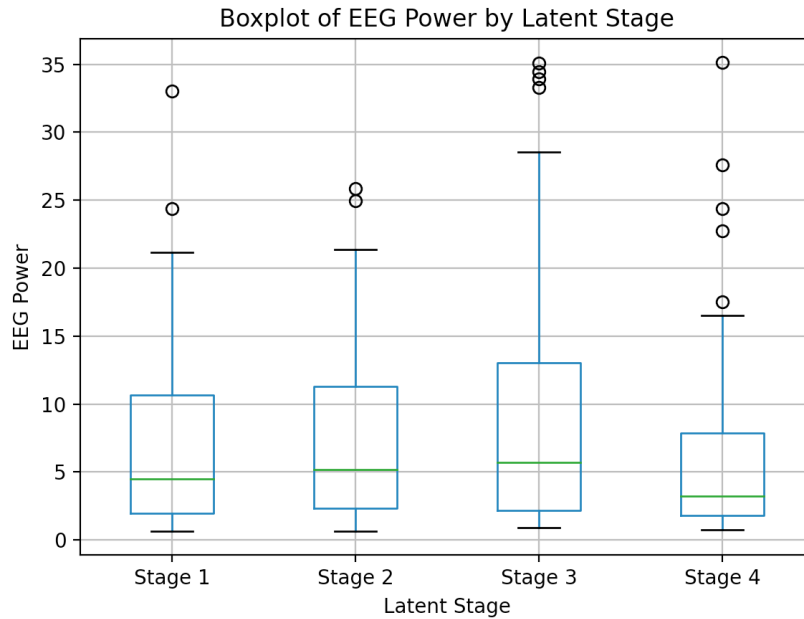


Figure 11. Boxplot of aggregated EEG power data from an exemplary feature across four latent stages

The Friedman test, followed by Conover's post-hoc comparisons, showed that the EEG power differences among latent cognitive stages were primarily pronounced within specific frequency bands of frontal areas, namely F7-theta, F4-beta, F4-gamma, F8-alpha. Significant pairwise differences, along with their respective effect sizes measured by Cohen's d , are delineated in Table 2. Notably, Stage 1 and Stage 2 were characterized by substantially lower theta band power at the F7 channel compared to Stage 3 (Stage 1 vs. Stage 3: $d = -0.81$, $p = 0.04$; Stage 2 vs. Stage 3: $d = -0.99$, $p = 0.03$), marking theta band power at F7 as a critical discriminator between these stages. Similar significant differences were observed in the beta and gamma bands at the F4 location and the alpha band at the F8 location across stages. Such consistent disparities across frontal channels highlights their potential relevance in characterizing the cognitive mechanisms involved in pedestrian road-crossing behavior. Visual depictions of these findings are presented through a boxplot (Figure 12) illustrating the spread and central tendencies of EEG power by stage, and a heatmap (Figure 13) that color-codes the statistical significance of stage-to-stage comparisons.

Table 2: Post-hoc pairwise comparisons of EEG measurements across conditions

Comparison	Test Statistic	p-value	Effect Size
Stage 1 vs. Stage 3 from F7- theta	-1.99	0.04	d= -0.81
Stage 2 vs. Stage 3 from F7- theta	-2.41	0.03	d= -0.99
Stage 1 vs. Stage 4 from F4- low beta	-2.09	0.02	d= -0.85
Stage 1 vs. Stage 4 from F4- high beta	-2.05	0.02	d= -0.84
Stage 2 vs. Stage 4 from F4- high beta	-1.59	0.04	d= -0.65
Stage 2 vs. Stage 4 from F4- gamma	-1.59	0.05	d= -0.65
Stage 2 vs. Stage 3 from F8- alpha	-2.25	0.04	d= -0.91
Stage 2 vs. Stage 4 from F8- alpha	-2.27	0.05	d= -0.93

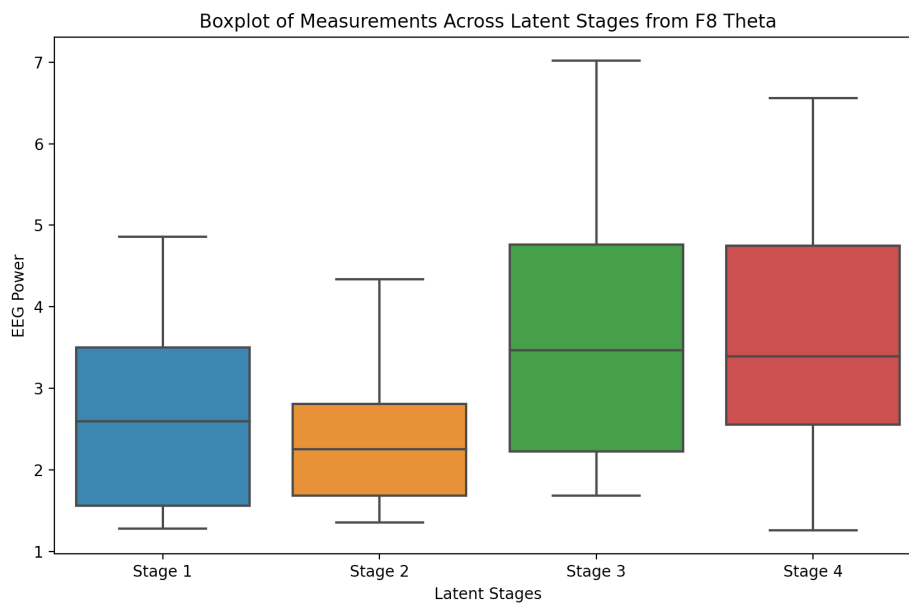


Figure 12. Boxplot of EEG Power Across Latent Stages from F8 Theta

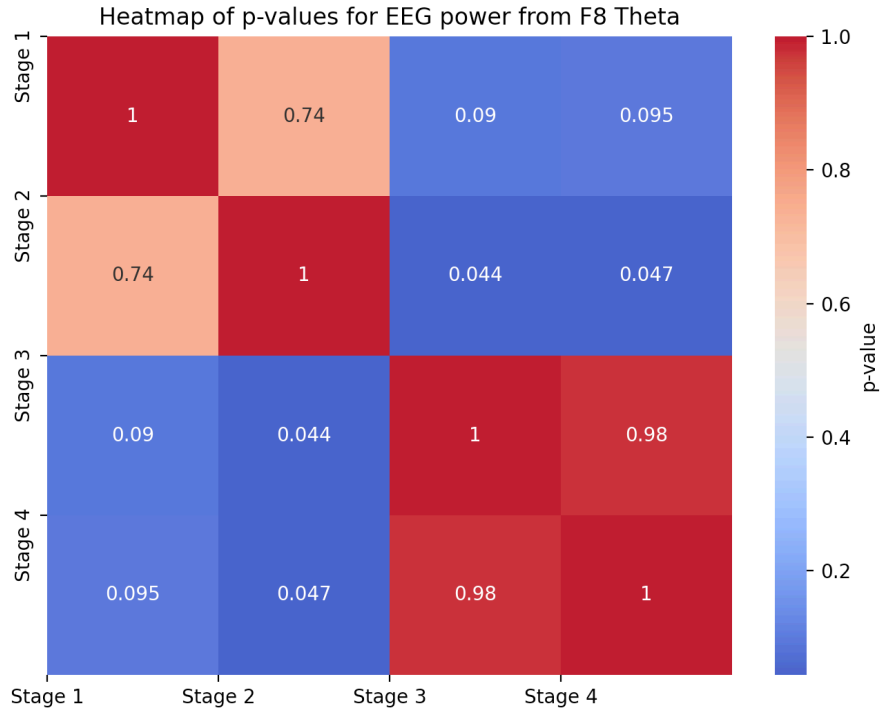


Figure 13. Heatmap of p-values across latent cognitive stages for EEG Power from F8 Theta

4.4 Classification Performance

Based on the statistical analyses results, we chose features from the F4-high beta frequency band as the discriminative proxy for predicting road-crossing intention. To further understand the impact of sliding window configuration on classification performance, we conducted a comparative analysis using various combinations of window length and stride. The results of this analysis, detailed in Table 3, demonstrate how subtle adjustments in the temporal segmentation can influence the model's ability to accurately classify EEG sequences. Receiver Operating Characteristic (ROC) curves were also generated (as shown in Figure 14) for each window configuration to provide a visual representation of the classifier's discriminative ability at various levels of sensitivity and specificity.

Table 3: Evaluation Metrics for Different Sliding Window Configurations at 8Hz sampling frequency

Window Length	Stride	The number of segments	Accuracy	Precision	Recall	F1 Score
5	9	326	0.76	0.59	0.70	0.59
8	9	304	0.83	0.51	0.57	0.5
9	3	838	0.80	0.51	0.60	0.48
11	7	356	0.83	0.53	0.72	0.52

In our investigation of EEG data related to decision-making processes for road-crossing,

we particularly focused on segments where the label '1' signifies the resolution of intention to cross the road, whereas instances labeled '0' represent periods during which subjects are still in the process of evidence accumulation before reaching a decision. By applying a sliding window with a preset length of 5 and a stride of 9, we segmented our time series data to capture these critical moments of cognitive transition.

As shown in Table 3, a combination of window length of 5 and a stride of 9 yielded the following performance metrics: an accuracy of 0.755, precision of 0.59, recall of 0.7, and an F1 score of 0.59. These results provide valuable insights into the model's ability to differentiate between the nuanced states of decision-making. The precision score highlights the model's effectiveness in accurately identifying true instances of decision resolution (label '1') amidst other cognitive processes. Meanwhile, a recall rate of 0.7 signifies the model's robust capability to capture a substantial majority of these critical decision-resolution moments, thus minimizing the risk of missing key instances of interest. The overall accuracy of 0.76 further affirms the model's efficiency across both classes, reinforcing its applicability in scenarios where distinguishing between ongoing decision-making and the resolution of decisions is crucial.

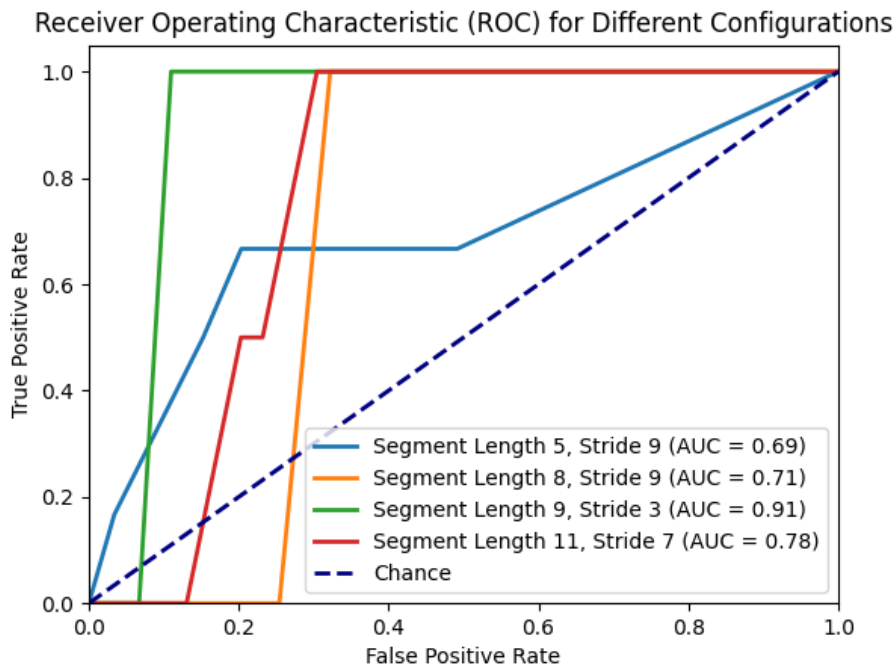


Figure 14. ROC Curves and AUC for Different Sliding Window Configurations

Furthermore, precision and recall are particularly sensitive to class imbalances and may not fully capture the trade-off between the True Positive Rate (TPR, or recall) and the False Positive Rate (FPR). Therefore, we employed ROC curves and the Area Under the Curve (AUC) to evaluate model performance across all possible classification thresholds. A high AUC indicates that the model can achieve a high TPR while maintaining a low FPR across various thresholds, not confined to a single operational point. We observed that a sliding window length of 9 with a stride of 3 yielded an AUC

of 0.91, despite precision and recall metrics being at modest levels. This underscores the model's discrimination capability. With optimized threshold selection and further model tuning, there is potential to further enhance the model's ability to distinguish between classes.

To verify the robustness of our model and to confirm that its predictions were not merely results of chance, we conducted a label shuffling test. In this test, the labels across the entire dataset were randomly shuffled while keeping the features unchanged, and then we performed five-fold cross-validation. Subsequently, the AUC metric, derived from the EEG features extracted using a sliding window of length 9 and stride 3, exhibited a significant decrease from an original value of 0.91 to 0.52. This decrease to approximately chance level after label shuffling (see Figure 15) highlights the genuine predictive capability of our model, demonstrating that its performance is not a product of random chance but rather a reflection of meaningful patterns captured from the EEG features.

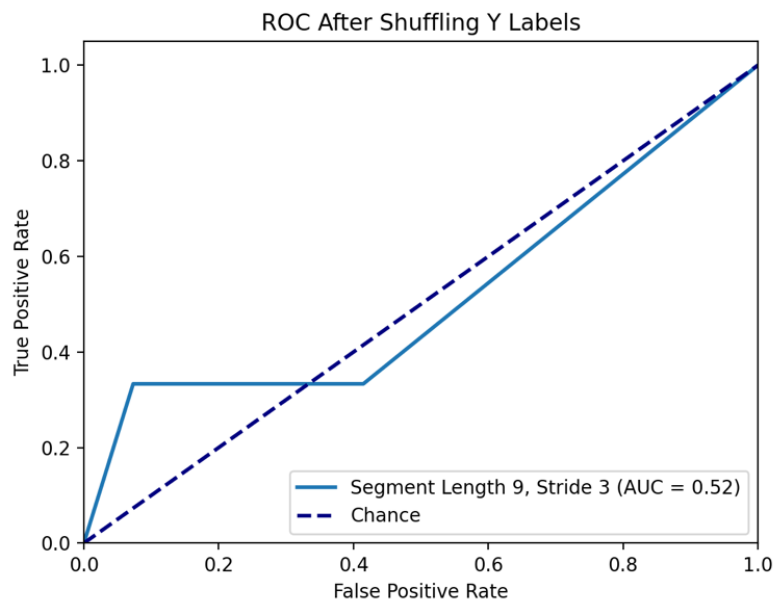


Figure 15. ROC Curve and AUC after label shuffling

5 Discussion

5.1 Cognitive States of Road-Crossing Behaviors

This study investigated the EEG correlates of the cognitive stages involved in road-crossing behavior. These patterns are indicative of the complexity of mental processes undertaken during the crossing decision, with each state possibly representing a different aspect of sensory processing, attention, decision planning or execution. Employing a data-driven approach via HMM, we discerned four distinct stages within the EEG data, which we tentatively aligned with the theoretical stages suggested by perceptual decision-making processes from psychology. Our statistical analyses revealed significant EEG activity differences among these stages, with theta and alpha activity reflecting early-stage perceptual processing and evidence accumulation, and

beta and gamma activity characterizing the later stages of decision resolution and execution.

5.1.1 Theta and Alpha Activity in Perception and Evidence Accumulation

The observed differences in theta activity at the F7 location between early-stage (perception) and later stages align with the theta frequency's established role in cognitive functions critical to initial perceptual processing [81]. Theta waves, particularly in frontal areas, have been linked to working memory [82] and selective attention [81]—key components in identifying and attending to relevant stimuli in complex environments like road crossings. The engagement of selective attention during the perception stage likely prepares the individual for the subsequent evidence evaluation, wherein working memory integrates incoming sensory information to inform decision-making.

The modulation of alpha activity at the F8 location further complements this cognitive framework. Alpha suppression, often observed in tasks requiring heightened attentional demand, suggests a release from inhibitory processes to facilitate the processing of relevant sensory information [83]. This dynamic might reflect the transition from a broad perceptual surveillance of the environment (perception) to a more focused evaluation of evidence necessary for making a safe crossing decision.

5.1.2 Beta and Gamma Activity in Decision Resolution and Execution

The final stage's distinction, primarily marked by beta and gamma activity at the F4 location, points toward the cognitive mechanisms underpinning decision resolution and execution. Beta frequency increases have been associated with the maintenance of current cognitive states [84], including sustained attention and working memory processes, which are imperative as one finalizes the crossing decision. Moreover, beta activity in the right frontal areas may underline the engagement of motor planning or anticipation mechanisms [85], preparing the individual for the physical act of crossing.

Gamma activity, known for its role in higher-order cognitive functions [86, 87], could signify the integration of accumulated evidence and the final decision-making processes. The increase in gamma band power might reflect the complex neural computations that consolidate sensory information, accumulated evidence, and potential outcomes into a decisive action plan—ultimately leading to the execution of the crossing behavior.

5.1.3 Implications and Future Research Directions

This research enriches our understanding of the neural underpinnings of pedestrian decision-making and offers a foundation for future studies to explore neurocognitive interventions or training programs aimed at enhancing pedestrian safety. Further investigation into the lateralization of brain activity and its relation to cognitive processes in decision-making can provide deeper insights into the mechanisms governing safe versus risky pedestrian behaviors.

By integrating our results with neuroscience literature, we not only validate the identified EEG correlates of decision-making stages in road-crossing contexts but also contribute to a broader comprehension of the neural dynamics of everyday cognitive tasks. Future research might extend this work by examining these cognitive stages in more diverse environments or populations, thereby uncovering the fundamental and specific aspects of pedestrian decision-making at the neural level.

5.2 Predictive Modeling of Road-Crossing Behavior from EEG Data and Its Applicability

In an effort to predict the precise moments of road-crossing behavior from EEG sequences, this study utilized DTW and KNN algorithms, capitalizing on the discriminative EEG features identified earlier. The extraction of EEG sequences was achieved through a sliding window technique. Our findings demonstrate that the configuration of the sliding window—specifically, a length of 9 and a stride of 3—emerged as most promising, yielding an AUC of 0.91. This high AUC signifies the model's strong capability to discriminate between instances of crossing and not crossing, based on continuously monitored EEG signals processed at a sampling rate of 8Hz. This implies that the model effectively utilizes EEG data from just over 1 second (9/8 seconds) to predict road-crossing behavior. This temporal window is crucial as it defines the lookahead time within which our model can anticipate a pedestrian's intention to cross, offering a tangible advance warning of about 1.125 seconds. We believe that this lead time is significant and can give AVs adequate time to react, which is critical as research investigating the takeover time for human drivers to regain situational awareness typically indicates a much higher requirement of approximately 2.7 seconds, according to the mean of a meta-analysis [88]. Thus, our model's quicker response capability could significantly enhance safety measures by reducing the likelihood of collisions and improve overall traffic flow by correctly and predictively interpreting right-of-way.

5.2.1 Modelling Considerations

The variations in classification performance obtained with different window configurations highlight the importance of finely tuning the temporal parameters used for feature extraction from EEG data. It highlights that the temporal granularity of EEG signals—how we segment and analyze these signals over time—can markedly influence the predictive power of machine learning models in capturing the nuanced patterns associated with cognitive tasks involving decision-making.

Moreover, the efficacy of DTW and KNN in this context suggests that these methods are particularly suited for handling the temporal variability and complexity of EEG data related to specific cognitive states or actions. DTW, by accounting for temporal distortions between sequences, and KNN, by leveraging the similarity among instances, together provide a robust framework for modeling time-series data where precise alignment and similarity of patterns are important.

5.2.2 Implications and Future Research Directions

In the burgeoning field of V2X communications [89], the capability to predict pedestrians' intentions to cross the road before the crossing action is initiated represents a pivotal advance, particularly within the Vehicle-to-Pedestrian (V2P) subset. The advent of V2P communication facilitated by our developed predictive cognitive models opens novel avenues for pedestrian-AV interactions. By integrating such predictive models to anticipate pedestrian actions, AVs can engage in proactive safety measures rather than reactive responses. This preemptive approach to pedestrian safety could dramatically reduce the incidence of accidents and near-misses, particularly in urban environments where pedestrians and vehicles share closely intertwined spaces. For instance, an AV could receive a signal indicating a pedestrian's intention to cross at an upcoming intersection while the pedestrian is in its occlusion zone or is seemingly distracted (e.g., looking at a mobile phone), and could slow down or alert the pedestrian, thereby enhancing safety proactively.

Overall, this research advances us towards a vision of the cognitive internet of road agents [90], where every participant—be it a vehicle, pedestrian, or infrastructure element—acts as a smart, interconnected node in a broader network of shared information. In this network, the flow of information is not merely mechanistic but facilitated with layers of cognitive processing, allowing for an adaptive and intelligent response system. Predictive models of pedestrian behavior, informed by neural processing and machine learning, become integral to this network, enabling a richer, more nuanced interaction among all road users.

Therefore, by bridging the gap between neuroscientific insights and machine learning, our study not only advances the field of cognitive neuroscience in understanding human cognitive behaviors in real-world scenarios, but also opens new horizons for applying these findings to real-world challenges in pedestrian safety and beyond. These promising results also inspire further exploration into several areas. Future work could investigate the scalability of this approach in more heterogeneous environments and explore pedestrian rolling behaviors or varied pedestrian demographics to assess its generalizability. Additionally, collaboration among researchers is encouraged to integrate these predictive models into wearable technologies or urban infrastructure to pave the way for practical applications aimed at improving pedestrian safety in real-time.

6 Conclusion

This study attempted to explore the predictive capabilities of EEG signals for anticipating pedestrian road-crossing intentions, situated within the broader context of V2X communications, specifically focusing on the V2P dynamic. By employing a data-driven approach through HMM to discern cognitive stages associated with pedestrian decision-making—perception, evidence accumulation, decision resolution, and execution—we have uncovered distinctive EEG patterns that correlate with these

cognitive processes. Our analysis revealed significant differences in EEG activity across these stages, particularly in theta and alpha bands during early decision-making phases and beta and gamma bands in later stages, providing neurophysiological insights into the cognitive mechanics of pedestrian behavior.

Our sliding window configuration for EEG sequence extraction, along with DTW and KNN algorithms, highlight the potential of such models to predict pedestrian actions with high accuracy, as evidenced by an AUC of 0.91. The practical implications of this research are of significance, marking a significant stride towards the realization of a fully connected and cognitive ecosystem of road agents. The integration of predictive models into AVs opens up new avenues for V2P communication, enabling vehicles to proactively adjust their actions based on real-time interpreted road-crossing intentions from pedestrians, thereby reducing the likelihood of collisions and enhancing road safety.

Looking ahead, this research paves the way for further exploration into the integration of wearables with V2X technologies. Challenges related to data privacy, system interoperability, and ethical considerations will need to be navigated as we advance. However, the potential to significantly enhance pedestrian safety and traffic management through the cognitive internet of road agents offers an exciting prospect for the future of urban transportation. With this vision, there are reasons to be optimistic about moving closer to creating safer, more efficient, and interconnected roadways for all users.

Acknowledgements

The authors would like to acknowledge the financial support for this research received from the United States Department of Transportation (USDOT) Center for Connected and Automated Transportation (CCAT) at the University of Michigan (Grant 69A3552348305), and from the US National Science Foundation (NSF) (Grant SCC-IRG 2124857). Any opinions and findings in this paper are those of the authors and do not necessarily represent those of the CCAT or NSF.

Conflicts of Interest

None

References

1. Huang, C., et al., *Human-Machine Adaptive Shared Control for Safe Driving Under Automation Degradation*. IEEE Intelligent Transportation Systems Magazine, 2021: p. 2-15.
2. Muhammad, K., et al., *Vision-Based Semantic Segmentation in Scene Understanding for Autonomous Driving: Recent Achievements, Challenges, and Outlooks*. IEEE Transactions on Intelligent Transportation Systems, 2022.
3. Levinson, J., et al., *Towards fully autonomous driving: Systems and algorithms*, in *Intelligent Vehicles Symposium (IV)*. 2011, IEEE Xplore. p. 163-168.
4. Lateef, F., M. Kas, and Y. Ruichek, *Motion and geometry-related information fusion through a*

- framework for object identification from a moving camera in urban driving scenarios. *Transportation Research Part C: Emerging Technologies*, 2023. **155**: p. 104271.
5. Ghorai, P., et al., *State Estimation and Motion Prediction of Vehicles and Vulnerable Road Users for Cooperative Autonomous Driving: A Survey*. *IEEE Transactions on Intelligent Transportation Systems*, 2022. **23**: p. 1-20.
 6. Goldhammer, M., et al., *Intentions of Vulnerable Road Users - Detection and Forecasting by Means of Machine Learning*. *IEEE Transactions on Intelligent Transportation Systems*, 2018.
 7. Deshmukh, A., et al., *A Systematic Review of Challenging Scenarios Involving Automated Vehicles and Vulnerable Road Users*. *Proceedings of the Human Factors and Ergonomics Society Annual Meeting*, 2023. **67**.
 8. Almodfer, R., et al., *Quantitative analysis of lane-based pedestrian-vehicle conflict at a non-signalized marked crosswalk*. *Transportation Research Part F Traffic Psychology and Behaviour*, 2015. **42**.
 9. Anaya, J., et al., *Vehicle to Pedestrian Communications for Protection of Vulnerable road Users*, in *IEEE Intelligent Vehicles Symposium (IV)*. 2014. p. 1037-1042.
 10. Administration, N.H.T.S., *Comparing Demographic Trends in Vulnerable Road User Fatalities and the U.S. Population, 1980–2019*. 2021.
 11. Organization, W.H. *Road traffic injuries*. 2023 [cited 2024 February 2]; Available from: <https://www.who.int/news-room/fact-sheets/detail/road-traffic-injuries>.
 12. Rothenbücher, D., et al. *Ghost driver: A field study investigating the interaction between pedestrians and driverless vehicles*. in *2016 25th IEEE International Symposium on Robot and Human Interactive Communication (RO-MAN)*. 2016.
 13. Keller, C. and D. Gavrila, *Will the Pedestrian Cross? A Study on Pedestrian Path Prediction*. *Intelligent Transportation Systems*, *IEEE Transactions on*, 2014. **15**: p. 494-506.
 14. Yeong, D.J., et al., *Sensor and Sensor Fusion Technology in Autonomous Vehicles: A Review*. *Sensors*, 2021. **21**: p. 2140.
 15. Pang, Y., et al., *Data-driven trajectory prediction with weather uncertainties: A Bayesian deep learning approach*. *Transportation Research Part C: Emerging Technologies*, 2021. **130**: p. 103326.
 16. Swargiary, M. and B.R. Kadali, *A study on meta-analysis approach for pedestrian-vehicle interaction using LiDAR*. *Transportation Engineering*, 2023. **13**: p. 100191.
 17. Rich, M. *Rolling Zettabytes: Quantifying the Data Impact of Connected Cars*. 2020 May 1, 2024]; Available from: <https://www.datacenterfrontier.com/connected-cars/article/11429212/rolling-zettabytes-quantifying-the-data-impact-of-connected-cars>.
 18. Godoy, J., et al., *A Grid-Based Framework for Collective Perception in Autonomous Vehicles*. *Sensors*, 2021. **21**: p. 744.
 19. Malik, S., et al., *Collaborative Perception—The Missing Piece in Realizing Fully Autonomous Driving*. *Sensors*, 2023. **23**.
 20. Wang, T.-H., et al., *V2VNet: Vehicle-to-Vehicle Communication for Joint Perception and Prediction*, in *Computer Vision – ECCV 2020*. 2020. p. 605-621.
 21. Chavhan, S., et al., *Edge-Empowered Communication-Based Vehicle and Pedestrian Trajectory Perception System for Smart Cities*. *IEEE Internet of Things Journal*, 2023.
 22. Kim, U.-H., et al., *A Real-time Vision Framework for Pedestrian Behavior Recognition and Intention Prediction at Intersections Using 3D Pose Estimation*. *ArXiv*, 2020. **abs/2009.10868**.

23. Noh, B., et al., *Analysis of Vehicle–Pedestrian Interactive Behaviors near Unsignalized Crosswalk*. Transportation Research Record: Journal of the Transportation Research Board, 2021. **2675**: p. 036119812199906.
24. Gandhi, T. and M. Trivedi, *Pedestrian Protection Systems: Issues, Survey, and Challenges*. IEEE Transactions on Intelligent Transportation Systems, 2007. **8**: p. 413-430.
25. Noh, B., et al., *Vision-Based Pedestrian’s Crossing Risky Behavior Extraction and Analysis for Intelligent Mobility Safety System*. Sensors, 2022. **22**: p. 3451.
26. Matsui, Y., et al., *Situations of Car-to-Pedestrian Contact*. Traffic injury prevention, 2013. **14**: p. 73-7.
27. Pool, E., J. Kooij, and D. Gavrilu, *Using road topology to improve cyclist path prediction*, in *IEEE Intelligent Vehicles Symposium (IV)*. 2017. p. 289-296.
28. Schneider, N. and D. Gavrilu, *Pedestrian Path Prediction with Recursive Bayesian Filters: A Comparative Study*, in *Proceedings of the 35th German Conference on Pattern Recognition*. 2013. p. 174-183.
29. Song, X., et al., *Pedestrian Trajectory Prediction Based on Deep Convolutional LSTM Network*. IEEE Transactions on Intelligent Transportation Systems, 2020: p. 1-18.
30. Rehder, E. and H. Kloeden, *Goal-Directed Pedestrian Prediction*, in *IEEE International Conference on Computer Vision Workshop (ICCVW)*. 2015. p. 139-147.
31. Bandyopadhyay, T., et al., *Intention-Aware Pedestrian Avoidance*. 2013: Experimental Robotics.
32. Alahi, A., et al., *Social LSTM: Human Trajectory Prediction in Crowded Spaces*, in *IEEE Conference on Computer Vision and Pattern Recognition (CVPR)*. 2016. p. 961-971.
33. Saleh, K., M. Hossny, and S. Nahavandi. *Intent prediction of vulnerable road users from motion trajectories using stacked LSTM network*. in *2017 IEEE 20th International Conference on Intelligent Transportation Systems (ITSC)*. 2017.
34. Saleh, K., M. Hossny, and S. Nahavandi, *Intent Prediction of Pedestrians via Motion Trajectories Using Stacked Recurrent Neural Networks*. IEEE Transactions on Intelligent Vehicles, 2018: p. 1-1.
35. Neogi, S., et al., *Context Model for Pedestrian Intention Prediction Using Factored Latent-Dynamic Conditional Random Fields*. IEEE Transactions on Intelligent Transportation Systems, 2020: p. 1-12.
36. Saleh, K., M. Hossny, and S. Nahavandi, *Contextual Recurrent Predictive Model for Long-Term Intent Prediction of Vulnerable Road Users*. IEEE Transactions on Intelligent Transportation Systems, 2019: p. 1-11.
37. Volz, B., et al., *A data-driven approach for pedestrian intention estimation*, in *IEEE 19th International Conference on Intelligent Transportation Systems (ITSC)*. 2016. p. 2607-2612.
38. Xu, H.R., et al., *Deep Learning-Based Pedestrian Detection Using RGB Images and Sparse LiDAR Point Clouds*. IEEE TRANSACTIONS ON INDUSTRIAL INFORMATICS, 2024.
39. Jiang, Z.C., et al., *A deep learning framework for detecting and localizing abnormal pedestrian behaviors at grade crossings*. NEURAL COMPUTING & APPLICATIONS, 2022. **34**(24): p. 22099-22113.
40. Gao, N., L. Zhao, and Ieee, *A Pedestrian Dead Reckoning System using SEMG based on Activities Recognition*, in *2016 IEEE CHINESE GUIDANCE, NAVIGATION AND CONTROL CONFERENCE (CGNCC)*. 2016. p. 2361-2365.
41. Liebner, M., F. Klanner, and C. Stiller, *Active safety for vulnerable road users based on*

- smartphone position data, in *Intelligent Vehicles Symposium (IV)*. 2013. p. 256-261.
42. Flach, A., et al., *Pedestrian Movement Recognition for Radio Based Collision Avoidance: A Performance Analysis*, in *Proceedings of the 73rd IEEE Vehicular Technology Conference*. 2011: Budapest, Hungary. p. 1-5.
 43. Datta, T., S. Jain, and M. Gruteser, *Towards City-Scale Smartphone Sensing of Potentially Unsafe Pedestrian Movements*, in *IEEE 11th International Conference on Mobile Ad Hoc and Sensor Systems (MASS)*. 2014. p. 663-667.
 44. Harle, R., *A Survey of Indoor Inertial Positioning Systems for Pedestrians*. IEEE COMMUNICATIONS SURVEYS AND TUTORIALS, 2013. **15**(3): p. 1281-1293.
 45. Andreone, L., et al., *Cooperative Systems for Vulnerable Road Users: The Concept of the WATCH-OVER Project*. 2006.
 46. Arena, F., G. Pau, and A. Severino, *V2X Communications Applied to Safety of Pedestrians and Vehicles*. Journal of Sensor and Actuator Networks, 2019. **9**: p. 3.
 47. Sugimoto, C., Y. Nakamura, and T. Hashimoto, *Prototype of pedestrian-to-vehicle communication system for the prevention of pedestrian accidents using both 3G wireless and WLAN communication*, in *3rd International Symposium on Wireless Pervasive Computing*. 2008, IEEE Xplore. p. 764-767.
 48. EMOTIV. *Brain-Computer Interface Guide*. 2024 [cited 2024 May 21]; Available from: https://www.emotiv.com/blogs/glossary/brain-computer-interface-guide?adgroupid=138768698289&campaignid=17057185126&device=c&gad_source=1&gclid=Cj0KCQjwLGYBhCYARIsAPqTz19gBBkKBVpj7mwJUNEZ2sH4mcFSTKbWH4iuauW6b56c8ECO2QCYy5IaArSoEALw_wcB&hsa_acc=5401365090&hsa_ad=644974459432&hsa_cam=17057185126&hsa_grp=138768698289&hsa_kw=emotiv&hsa_mt=p&hsa_net=adwords&hsa_src=g&hsa_tgt=kwd-315386528571&hsa_ver=3&network=g&utm_campaign=Brand&utm_content=644974459432&utm_medium=ppc&utm_source=google&utm_term=emotiv.
 49. Churchland, A.K., R. Kiani, and M.N. Shadlen, *Decision-making with multiple alternatives*. Nature Neuroscience, 2008. **11**(6): p. 693-702.
 50. Gold, J. and M. Shadlen, *The Neural Basis of Decision Making*. Annual review of neuroscience, 2007. **30**: p. 535-74.
 51. Kable, J.W. and P.W. Glimcher, *The Neurobiology of Decision: Consensus and Controversy*. Neuron, 2009. **63**(6): p. 733-745.
 52. O'Connell, R.G., P.M. Dockree, and S.P. Kelly, *A supramodal accumulation-to-bound signal that determines perceptual decisions in humans*. Nature Neuroscience, 2012. **15**(12): p. 1729-1735.
 53. Kubanek, J., et al., *Cortical alpha activity predicts the confidence in an impending action*. Frontiers in Neuroscience, 2015. **9**.
 54. Fleury, M., et al., *Two is better? Combining EEG and fMRI for BCI and neurofeedback: a systematic review*. Journal of Neural Engineering, 2023. **20**.
 55. Bressler, S.L., *Understanding Cognition Through Large-Scale Cortical Networks*. Current Directions in Psychological Science, 2002. **11**(2): p. 58-61.
 56. Dickhaus, T., et al., *Predicting BCI performance to study BCI illiteracy*. BMC Neuroscience, 2009. **10**(1): p. 84.
 57. Islam, M., et al., *Cognitive State Estimation by Effective Feature Extraction and Proper*

- Channel Selection of EEG Signal*. Journal of Circuits System and Computers, 2015. **24**.
58. Gundel, A. and G.F. Wilson, *Topographical changes in the ongoing EEG related to the difficulty of mental tasks*. Brain Topography, 1992. **5**(1): p. 17-25.
 59. Pavlov, A., et al., *Recognition of electroencephalographic patterns related to human movements or mental intentions with multiresolution analysis*. Chaos, Solitons & Fractals, 2019. **126**: p. 230-235.
 60. Kowalski-Trakofler, K.M. and E.A. Barrett, *The concept of degraded images applied to hazard recognition training in mining for reduction of lost-time injuries*. Journal of Safety Research, 2003. **34**(5): p. 515-525.
 61. Windridge, D., A. Shaukat, and E. Hollnagel, *Characterizing Driver Intention via Hierarchical Perception–Action Modeling*. IEEE Transactions on Human-Machine Systems, 2013. **43**(1): p. 17-31.
 62. Ptak, R., *The Frontoparietal Attention Network of the Human Brain: Action, Saliency, and a Priority Map of the Environment*. Neuroscientist, 2012. **18**(5): p. 502-515.
 63. Desimone, R., *Neural Mechanisms of Selective Visual Attention*. Annual Review of Neuroscience, 1995. **18**: p. 193-222.
 64. Vossel, S., J. Geng, and G. Fink, *Dorsal and Ventral Attention Systems: Distinct Neural Circuits but Collaborative Roles*. The Neuroscientist : a review journal bringing neurobiology, neurology and psychiatry, 2013. **20**.
 65. Bressler, S., et al., *Top-Down Control of Human Visual Cortex by Frontal and Parietal Cortex in Anticipatory Visual Spatial Attention*. The Journal of neuroscience : the official journal of the Society for Neuroscience, 2008. **28**: p. 10056-61.
 66. Bunge, S.A., *How we use rules to select actions: a review of evidence from cognitive neuroscience*. Cognitive, Affective & Behavioral Neuroscience, 2005. **4**: p. 564-579.
 67. Galeano-Keiner, E., et al., *Distributed patterns of occipito-parietal functional connectivity predict the precision of visual working memory*. NeuroImage, 2016. **146**.
 68. Olszewski, P., et al., *Pedestrian fatality risk in accidents at unsignalized zebra crosswalks in Poland*. Accident Analysis & Prevention, 2015. **84**: p. 83-91.
 69. Haleem, K., P. Alluri, and A. Gan, *Analyzing pedestrian crash injury severity at signalized and non-signalized locations*. Accident Analysis & Prevention, 2015. **81**: p. 14-23.
 70. Fu, T., et al., *Investigating secondary pedestrian-vehicle interactions at non-signalized intersections using vision-based trajectory data*. Transportation Research Part C: Emerging Technologies, 2019. **105**: p. 222-240.
 71. Noh, B., et al. *Vision-Based Potential Pedestrian Risk Analysis on Unsignalized Crosswalk Using Data Mining Techniques*. Applied Sciences, 2020. **10**, DOI: 10.3390/app10031057.
 72. Koehler, S., et al., *Stationary Detection of the Pedestrian's Intention at Intersections*. IEEE Intelligent Transportation Systems Magazine, 2013. **5**(4): p. 87-99.
 73. Peirce, J., et al., *PsychoPy2: Experiments in behavior made easy*. Behavior Research Methods, 2019. **51**(1): p. 195-203.
 74. EMOTIV. *EPOC X Coverage*. 2020 [cited 2023 December fourteenth]; Available from: <https://emotiv.gitbook.io/epoc-x-user-manual/introduction/introduction-to-epoc-x/coverage>.
 75. EMOTIV. *EmotivPRO v3.0*. 2023 [cited 2023 December fourteenth]; Available from: <https://emotiv.gitbook.io/emotivpro-v3/data-streams/frequency-bands>.
 76. Cochran, W., et al., *What is the fast Fourier transform?* Proceedings of the IEEE, 1967. **15**: p.

- 1664-1674.
77. Yu, X., P. Chum, and K.-B. Sim, *Analysis the effect of PCA for feature reduction in non-stationary EEG based motor imagery of BCI system*. Optik, 2014. **125**: p. 1498-1502.
 78. Poritz, A., *Hidden Markov models: A guided tour*, in *International Conference on Acoustics, Speech, and Signal Processing*. 1988, IEEE Xplore. p. 7-13 vol.1.
 79. He, H., et al., *ADASYN: Adaptive Synthetic Sampling Approach for Imbalanced Learning*, in *IEEE International Joint Conference on Neural Networks*. 2008. p. 1322-1328.
 80. Müller, M., *Dynamic time warping*. Information Retrieval for Music and Motion, 2007. **2**: p. 69-84.
 81. Karakaş, S., *A review of theta oscillation and its functional correlates*. International Journal of Psychophysiology, 2020.
 82. Raghavachari, S., et al., *Gating of Human Theta Oscillations by a Working Memory Task*. The Journal of Neuroscience, 2001. **21**(9): p. 3175-3183.
 83. Foxe, J. and A. Snyder, *The Role of Alpha-Band Brain Oscillations as a Sensory Suppression Mechanism during Selective Attention*. Frontiers in Psychology, 2011. **2**(154).
 84. Engel, A.K. and P. Fries, *Beta-band oscillations—signalling the status quo?* Current Opinion in Neurobiology, 2010. **20**(2): p. 156-165.
 85. Wagner, J., et al., *Establishing a Right Frontal Beta Signature for Stopping Action in Scalp Electroencephalography: Implications for Testing Inhibitory Control in Other Task Contexts*. Journal of cognitive neuroscience, 2017. **30**: p. 1-12.
 86. Jensen, O., J. Kaiser, and J.-P. Lachaux, *Human gamma-frequency oscillations associated with attention and memory*. Trends in neurosciences, 2007. **30**: p. 317-24.
 87. Polanía, R., W. Paulus, and M. Nitsche, *Noninvasively Decoding the Contents of Visual Working Memory in the Human Prefrontal Cortex within High-gamma Oscillatory Patterns*. Journal of cognitive neuroscience, 2012. **24**: p. 304-14.
 88. Zhang, B., et al., *Determinants of take-over time from automated driving: A meta-analysis of 129 studies*. Transportation Research Part F: Traffic Psychology and Behaviour, 2019. **64**: p. 285-307.
 89. Paden, B., et al., *A Survey of Motion Planning and Control Techniques for Self-Driving Urban Vehicles*. IEEE Transactions on Intelligent Vehicles, 2016. **1**.
 90. Chen, M., et al., *Cognitive Internet of Vehicles*. Computer Communications, 2018. **120**: p. 58-70.